

Cholesteric pitch transitions induced by mechanical strain

Original

Cholesteric pitch transitions induced by mechanical strain / I., Lelidis; Barbero, Giovanni; A. L., Alexe Ionescu. - In: PHYSICAL REVIEW E, STATISTICAL, NONLINEAR, AND SOFT MATTER PHYSICS. - ISSN 1539-3755. - 87:(2013), pp. 022503-1-022503-7. [10.1103/PhysRevE.87.022503]

Availability:

This version is available at: 11583/2507609 since:

Publisher:

American Physical Society (APS)

Published

DOI:10.1103/PhysRevE.87.022503

Terms of use:

This article is made available under terms and conditions as specified in the corresponding bibliographic description in the repository

Publisher copyright

(Article begins on next page)

Cholesteric pitch transitions induced by mechanical strain

I. Lelidis,^{1,2,3} G. Barbero,^{2,3} and A. L. Alexe-Ionescu^{2,4}

¹*Solid State Section, Department of Physics, University of Athens, Panepistimiopolis, Zografos, Athens 157 84, Greece*

²*Department of Applied Science and Technology, Politecnico di Torino, Corso Duca degli Abruzzi 24, 10129 Torino, Italia*

³*Université de Picardie Jules Verne, Laboratoire de Physique des Systèmes Complexes, 33 rue Saint-Leu, 80039 Amiens, France*

⁴*University Politehnica of Bucharest, Faculty of Applied Sciences, Splaiul Independentei 313, 060042 Bucharest, Romania*

(Received 18 October 2012; published 13 February 2013)

We investigate thickness and surface anchoring strength influence on pitch transitions in a planar cholesteric liquid crystal layer. The cholesteric-nematic transition is also investigated. We assume planar boundary conditions, with strong anchoring strength at one interface and weak anchoring strength at the other. The surface anchoring energy we consider to describe the deviation of the surface twist angle from the easy axis induced by a bulk deformation is a parabolic potential or Rapini and Papoular periodic potential, respectively. We show that under strain, all pitch transitions take place at a critical thickness that is equal to the quarter of the natural cholesteric pitch. The latter result does not depend on the anchoring strength, the particular surface potential, or material properties. The twist angle on the limiting surface characterized by weak anchoring varies with strain either by slipping and or in a discontinuous manner according to the thickness of the sample. The position of the bifurcation point depends only on the ratio of the extrapolation length over the layer thickness, but its value is model dependent. Multistability and multiplicity of the transition are discussed.

DOI: [10.1103/PhysRevE.87.022503](https://doi.org/10.1103/PhysRevE.87.022503)

PACS number(s): 64.70.M-, 61.30.Dk

I. INTRODUCTION

The effect of an external field on a unbounded cholesteric liquid crystal (CLC) has been discussed long ago by de Gennes [1] and independently by Meyer [2]. They saw that the presence of a magnetic field is responsible for a continuous increasing of the pitch of the CLC. The pitch diverges when the external field reaches a critical value that depends on the magnetic and elastic properties of the CLC. The analysis has been extended to a sample of finite thickness by Dreher [3] and Stewart *et al.* [4,5], who predicted that the pitch increases by finite steps, due to the boundary conditions imposed on the limiting surfaces. According to their analysis, the CLC expels a pitch all the time the external field reaches well defined critical values. Pitch transitions in a CLC can also be induced by the variation of the temperature that influences the intrinsic periodicity of the CLC. Temperature-induced pitch transitions have been investigated by Belyakov *et al.* [6–8] and Palto [9]. The instability mechanism underlying the pitch transitions has been discussed by Kiselev and Sluckin in [10]. Recently, Scarfone *et al.* [11,12] have shown that in the limit of infinite thickness the analysis presented in [3,4] yields the results reported in [1]. Experimental observations of CLC pitch transitions have been reported in [13–18].

Under the presence of an external field, magnetic or electric, the nematic director tends to orient parallel or perpendicular to the applied field direction, according to the diamagnetic or dielectric anisotropy of the CLC [19,20]. In order to minimize the total energy, including both elastic and external bulk field contributions, the CLC distorts its structure up to destroy its intrinsic periodicity [3,11]. In the present paper, we investigate the effect of the sample thickness in conjunction with the anchoring strength on the CLC pitch transitions. In the case that anchoring is strong enough, reducing the thickness of the sample, the CLC has to pay a price in elastic energy to maintain its natural periodicity. As soon as this price becomes too large, the CLC expels a half pitch in order to avoid divergences in the

elastic energy contribution. Our aim is to analyze the role of the surface anchoring, taking into account the direct interaction between the CLC and the limiting surfaces, in this instability. We assume that the surface energy (i) is proportional to the square of the deviation of the actual surface twist angle from the easy direction imposed by the surface treatment (parabolic potential) or (ii) is well approximated by the functional form proposed by Rapini and Papoular [21]. In both cases we show that reducing the thickness of the sample, the surface twist angle is slipping to reduce the strain elastic energy of the confined CLC or/and is presenting discontinuous variations as soon as the thickness reaches a well defined value that depends on the elastic and surface properties of the sample. Finally, we show that the position of the critical point between the two regimes is model dependent and therefore it could be used in order to determine the most adequate surface potential.

II. THE MODEL SYSTEM

We consider a CLC confined between two infinite parallel plates with spacing d . The Cartesian reference frame used for the description has the z axis perpendicular to the plates, with the bounding surfaces located at $z = 0$ and $z = d$. Both plates are supposed to induce planar alignment, with the easy direction \mathbf{e} along the x axis. The interface at $z = 0$ is assumed with infinitely strong anchoring, whereas the one at $z = d$ is assumed with finite azimuthal anchoring energy. The nematic director \mathbf{n} , describing the average molecular orientation, is assumed to be everywhere parallel to the (x, y) plane even in the strained state. The angle formed by \mathbf{n} with the x axis is indicated by $\phi(z)$. The helical axis is in the z direction. The total energy per unit area of the sample is given by

$$F = \frac{K}{2} \int_0^d \left(\frac{d\phi}{dz} - \frac{\pi}{\lambda_0} \right)^2 dz + f_s(\mathbf{n}, \mathbf{e}), \quad (1)$$

where K is the twist elastic constant, λ_0 the natural half-pitch of the CLC, and f_s the surface energy describing the anisotropic part of the surface tension at the upper ($z = d$) CLC-substrate interface.

Our aim is to examine the influence of the slab thickness and of the anchoring strength on the CLC helix unwinding when f_s is approximated by (i) a parabolic potential, and (ii) a periodic potential of the Rapini and Papoular form [21]. We use two forms for the surface anchoring energy in order to investigate if the main features of the pitch transitions are model dependent.

In case (i), f_s has the form

$$f_s = \frac{w}{2}(\phi_s - \phi_e)^2, \quad (2)$$

where w is the anchoring energy strength, $\phi_s = \phi(z = d)$ the twist angle at the upper-interface, and ϕ_e the easy angle between \mathbf{e} and the x axis. Due to the symmetry of the CLC phase, the easy angle is a multiple of π ; i.e., in the frame of the present model system, $\phi_e^N = N\pi$ for a unstrained cell that contains N half pitch (of thickness $d_0 = N\lambda_0$). The parabolic potential as it is introduced by Eq. (2) is not a π -periodic potential. In the case (ii), the surface energy has the functional form $f_s = (w/2)\sin^2(\phi_s - \phi_e)$, proposed by Rapini and Papoular [21]. Since $\phi_e = m\pi$, where m is an integer, f_s reads

$$f_s = \frac{w}{2}\sin^2\phi_s. \quad (3)$$

III. PARABOLIC POTENTIAL

To investigate the influence of the thickness of the sample on the CLC structure it is necessary to find the dependence of the twist angle $\phi(z)$ on d . By minimizing F given by Eq. (1) we get $d^2\phi/dz^2 = 0$, from which it follows that $\phi(z) = \phi_s(z/d)$, where we have taken into account that $\phi(0) = 0$ from the hypothesis of strong anchoring on the surface at $z = 0$. By substituting the latter expression into Eq. (1) we obtain for the rescaled energy $G = 2F/K$ the expression

$$G = \left(\frac{\phi_s}{d} - \frac{\pi}{\lambda_0}\right)^2 d + \frac{(\phi_e - \phi_s)^2}{L}, \quad (4)$$

where $L = K/w$ is the extrapolation length [22]. Equation (4) gives $G = G(\phi_s)$. The actual ϕ_s is determined by minimizing $G(\phi_s)$ with respect to ϕ_s . From Eq. (4) we get

$$G' = \frac{dG}{d\phi_s} = 2\left\{\left(\frac{\phi_s}{d} - \frac{\pi}{\lambda_0}\right) - \frac{\phi_e - \phi_s}{L}\right\}, \quad (5)$$

$$G'' = \frac{d^2G}{d\phi_s^2} = 2\left(\frac{1}{d} + \frac{1}{L}\right). \quad (6)$$

The condition $G' = 0$ gives

$$\phi_s = \frac{Ld}{d+L}\left(\frac{\pi}{\lambda_0} + \frac{\phi_e}{L}\right), \quad (7)$$

relating ϕ_s to the thickness of the sample d . This solution is always stable, since $G'' > 0$ for all ϕ_e , as it follows from Eq. (6). From Eq. (7) one obtains d in terms of the surface

twist angle, ϕ_s , minimizing G :

$$d = \frac{\phi_s}{\pi/\lambda_0 + (\phi_e - \phi_s)/L}. \quad (8)$$

By substituting Eq. (7) into Eq. (4) we get

$$G = \frac{d^2}{d+L}\left(\frac{\phi_e}{d} - \frac{\pi}{\lambda_0}\right)^2, \quad (9)$$

giving G versus the external field d and the easy direction ϕ_e . First, let us consider $\phi_e = N\pi$; $N = 0, 1, 2, \dots, N_{\max}$. In this case, the surface twist angle ϕ_s is indicated by Φ_N and Eq. (7) reads

$$\Phi_N = \frac{Ld}{d+L}\left(\frac{1}{\lambda_0} + \frac{N}{L}\right)\pi. \quad (10)$$

From Eq. (10) it follows that when d decreases, Φ_N decreases too. From Eq. (9) the total energy can be rewritten as

$$G_N = \left(N - \frac{d}{\lambda_0}\right)^2 \frac{\pi^2}{d+L} \geq 0 \quad (11)$$

and it follows that G_N has a minimum at any $d_0 = N\lambda_0$, where it vanishes.

The condition for a pitch transition between two states that differ by a half-pitch number ΔN ($N \leftrightarrow N + \Delta N$ pitch transition) is given by the equality of the total energy of the two configurations

$$G_N = G_{N+\Delta N} \Rightarrow d_c(N, \Delta N) = \left(N + \frac{\Delta N}{2}\right)\lambda_0. \quad (12)$$

Note that, from the latter condition for the transition, the critical thickness $d_c(N, \Delta N)$ does not depend on anchoring or on material properties, and, therefore, it is purely topological. The values of $\Delta N = \pm 1, \pm 2, \dots$ are subjected to the condition that the thickness is a positive real number. The absolute value of ΔN is the multiplicity m_p of the transition ($m_p = |\Delta N|$). Transitions between stable states have always $m_p = 1$. Transitions with $m_p > 1$ involve metastable states and at most one stable state.

Figure 1 shows G_N vs d , for $L/\lambda_0 = 1$. The energy curves intersect always at $(N \pm 1/2)\lambda_0$ or $N\lambda_0$. If the half-pitch number N is conserved above the intersection point of successive energy curves, the system enters the metastable states indicated by dashed lines in Fig. 1. For instance, in a cell with initially $N = 10$ that is strained, the transition $10 \rightarrow 9$ could happen at the point A where the two configurations have the same energy. If the system is blocked at the state $N = 10$ above A , then it becomes metastable and it could attain the point B , if it does not relax in between, where a transition $10 \rightarrow 8$ may happen. Of course, a transition $10 \rightarrow 9$ remains always probable even if the system has reached the cross point B . This kind of bistability has also been predicted for the RP potential in [10]. Transitions where the initial strained state may relax towards three different states (tristability) are also possible; e.g., see in Fig. 1 the energy curve for $N = 11$, if the system crosses the point C it can relax towards three configurations with $N = 8, 9, 10$, etc. To reach this kind of multistability the system has to be trapped in a state with high enough energy. At this point, it is useful to introduce the number $m_s = 1, 2, \dots$ that characterizes the

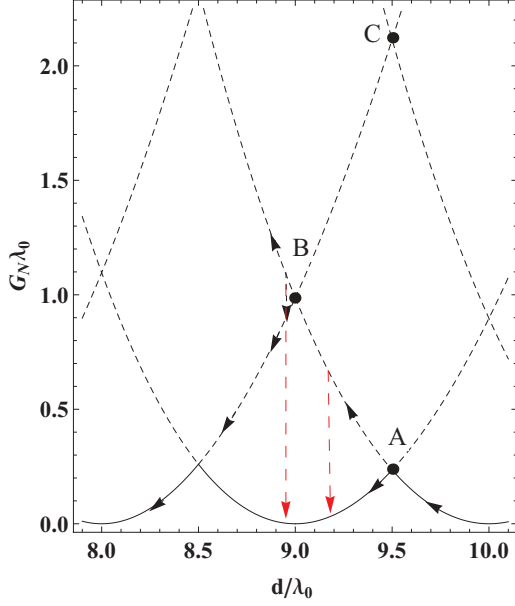


FIG. 1. (Color online) Energy vs d/λ_0 . The CLC pitch transition takes place at the crossing point between successive energy curves. Above the crossing points of the energy curves the system enters in the range of metastable states (dashed lines). Vertical arrows indicate transitions from a metastable state towards another metastable (black arrows) or a stable state (red arrows).

order of multistability. In absence of multistability $m_s = 1$. Note that multiplicity and multistability are permitted because the parabolic potential is not assumed to be periodic.

The energy barrier $\Delta G = G(N - 1/2) - G(N, d)$ between successive stable CLC states ($m_s = 1$), as function of the cell thickness is plotted in Fig. 2, for $L/\lambda_0 = 0, 10, 100$. In general, the energy $G(N, d)$ of the initial state depends on the sample thickness. For an unstrained system ($d = N\lambda_0$) the energy vanishes $G(N, N\lambda_0) = 0$. As it is shown, the energy

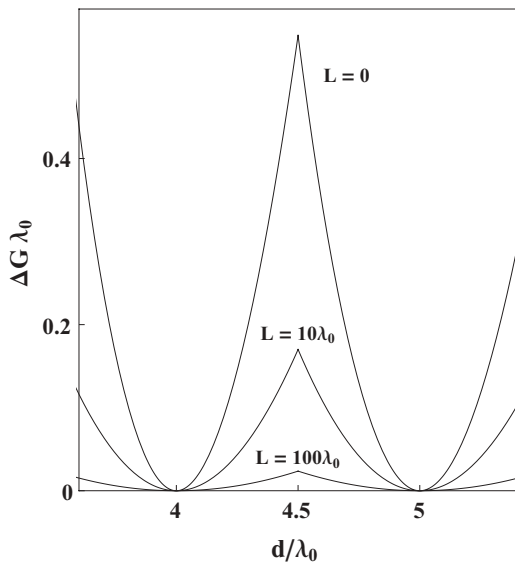


FIG. 2. The energy barrier $\Delta G \lambda_0$ between successive CLC states vs d/λ_0 ($m_s = 1$). For increasing values of L the energy barrier is decreasing. If the cell is prestrained the energy barrier decreases.

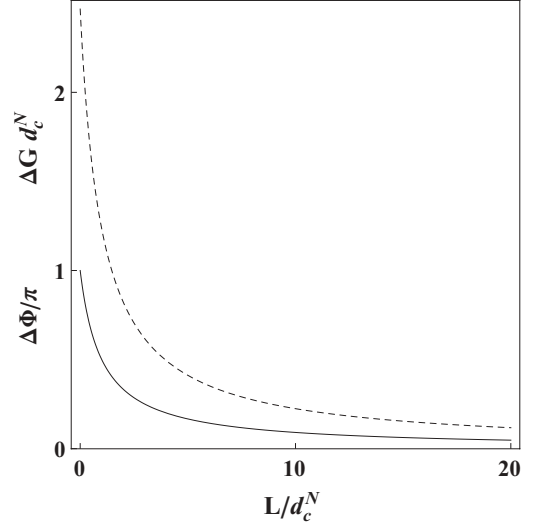


FIG. 3. The energy barrier $\Delta G d_c^N$ (dashed line) and surface twist angle jump (continuous line) $\Delta\Phi$ between successive CLC states vs L/d_c^N . $m_s = 1$.

barrier increases when the extrapolation length decreases. Figure 3 shows the energy barrier ΔG for an initially unstrained system, dashed line, at the transition vs L/d_c^N with $d_c^N = d_c(N, \pm 1)$. The energy barrier of the $N \leftrightarrow N - 1$ pitch transition increases with the relative anchoring strength, i.e., decreasing L and increasing N .

The surface twist angle at the critical thickness is given by

$$\Phi(d_c^N) = \frac{(2N - 1)(L + N\lambda_0)}{2L + (2N - 1)\lambda_0}, \quad (13)$$

$$\pi = N\pi \frac{1 + L/(N\lambda_0)}{1 + L/d_c^N}.$$

The latter equation shows that $\Phi(d_c^N)$ is an increasing function of N . At the cholesteric-nematic (Ch-N) transition $\Phi(d_c^N)$ varies from π for strong anchoring ($\lambda_0 \gg L$) towards $\pi/2$ for weak enough anchoring ($\lambda_0 \ll L$).

The jump of the surface twist angle at d_c^N is written as

$$\Delta\Phi = \frac{(2N - 1)\pi\lambda_0}{2L + (2N - 1)\lambda_0} = \frac{\pi}{1 + L/d_c^N}. \quad (14)$$

For $L = 0$, $\Delta\Phi = \pi$ and for $L = \infty$, $\Delta\Phi = 0$. In Fig. 3 is also reported the dependence of the surface twist angle discontinuity $\Delta\Phi$ at the transition on L/d_c^N (continuous line). As it is shown the amplitude of $\Delta\Phi$ depends on the extrapolation length L and the number of half twist turns in the cell. Combining Eqs. (13) and (14), one finds that the relative surface twist angle variation at the pitch transition

$$\frac{\Delta\Phi}{\Phi} = \frac{1}{N + L/\lambda_0} \quad (15)$$

decreases with the order N of the transition.

Finally, Fig. 4 shows the surface twist angle variation with the thickness of the CLC cell for three values of the extrapolation length, $L/\lambda_0 = 0.001, 1, 10$. The discontinuity $\Delta\Phi$ of ϕ_s appears at the pitch transitions and increases with N at constant L . For the same N , the jump increases with the anchoring strength w .

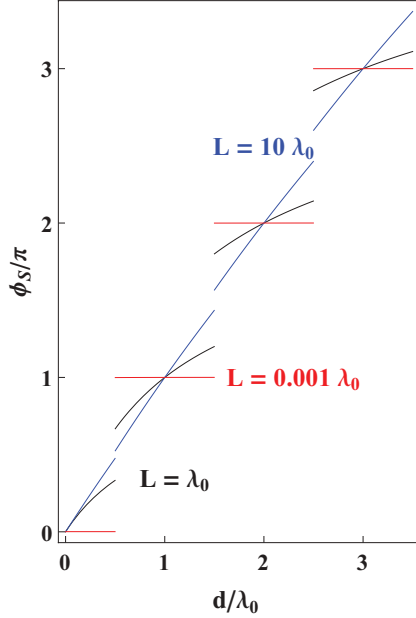


FIG. 4. (Color online) Variation of the surface twist angle ϕ_s in units of π with d/λ_0 for $L/\lambda_0 = 0.001, 1, 10$. $m_s = 1$. The jump of ϕ_s at the transition is increasing with N while decreasing with L .

In conclusion, the parabolic potential predicts that for finite L there is always a discontinuity of the surface twist angle at the pitch transition of any order. For $L = \infty$ the transition is continuous and independent of the thickness value ($d \neq 0$); i.e., there is a critical point (CP) at infinity. However, the system never becomes unstable [see Eq. (6)]. If the system is blocked in a metastable state, then multiple half pitch transitions may take place (see Fig. 1) as experimentally observed in [13]. The critical thickness for the complete unwinding $N = 1 \rightarrow 0$ transition is calculated from Eq. (12), as $d_c = \lambda_0/2$ in accordance to the prediction of [11].

IV. RAPINI-PAPOULAR POTENTIAL

If the anchoring energy is assumed of Rapini-Papoular form, the rescaled energy $G = 2F/K$ of the CLC is

$$G = \left(\frac{\phi_s}{d} - \frac{\pi}{\lambda_0} \right)^2 d + \frac{1}{L} \sin^2 \phi_s. \quad (16)$$

Minimization of the energy ($G' = 0$) leads to the dependence of the cell thickness on the surface twist angle that extremizes $G(\phi_s, d)$

$$\frac{d}{\lambda_0} = \frac{\phi_s}{\pi} \frac{1}{1 - \lambda_0 \sin 2\phi_s / (2\pi L)}. \quad (17)$$

The latter equation also gives the surface twist angle as a function of the thickness of the cell in implicit form. This relation is of some practical importance since in experiments d plays the role of the external field. Figure 5 shows the surface twist angle as function of the cell thickness. The diagonal dashed line corresponds to $L = \infty$ while the bold continuous sigmoidal line corresponds to $L = \lambda_0$. Note that for finite values of L , $\phi_s(d)$ presents strong nonlinearities for $d > L$. From $G' = 0$, the energy of the strained CLC as function of

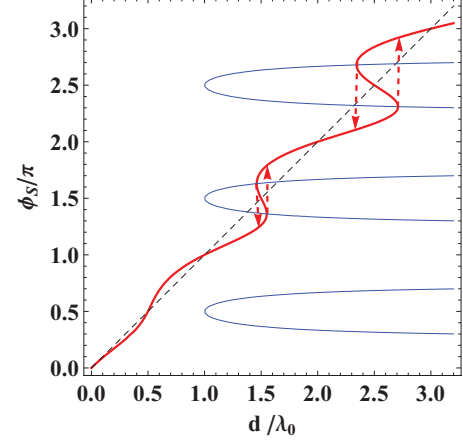


FIG. 5. (Color online) ϕ_s vs d/λ_0 for $L = \infty$, dashed line, and $L = \lambda_0$, continuous line. The blue curves correspond to the spinodal of the system for $L = \lambda_0$.

ϕ_s is cast in the form

$$G(\phi_s) = \frac{\sin^2 \phi_s}{L} \left(1 + \phi_s \frac{1 + \cos 2\phi_s}{(2\pi L/\lambda_0) - \sin 2\phi_s} \right) \geq 0. \quad (18)$$

Figure 6 shows G as function of ϕ_s , for $L = \lambda_0$. The energy has absolute minima at $\phi_s = N\pi$, where it takes the value $G(N\pi) = 0$. At $\phi_s = (2N - 1)\pi/2$, G has a local minimum if $L < d$. The latter extremum becomes an absolute maximum when $L > d$. In both cases, for $\phi_s = (2N - 1)\pi/2$ one gets $G = 1/L$. The dependence of G on ϕ_s given by Eq. (18) implies, in general, intervals of continuous variation of ϕ_s separated by first order transitions when d is varied.

The thermodynamical stability of the system, $G'' \geq 0$, is given by the spinodal line

$$1 + \frac{d}{L} \cos 2\phi_s = 0. \quad (19)$$

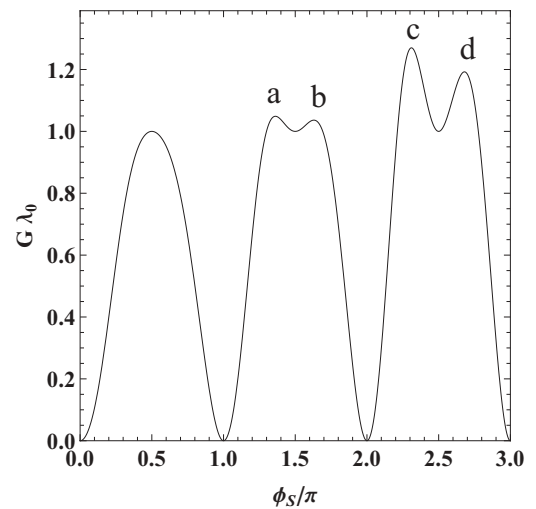


FIG. 6. CLC energy vs surface twist angle, for $L = \lambda_0$. The part of the curve between the maxima a and b (c and d) represents metastable and unstable states.

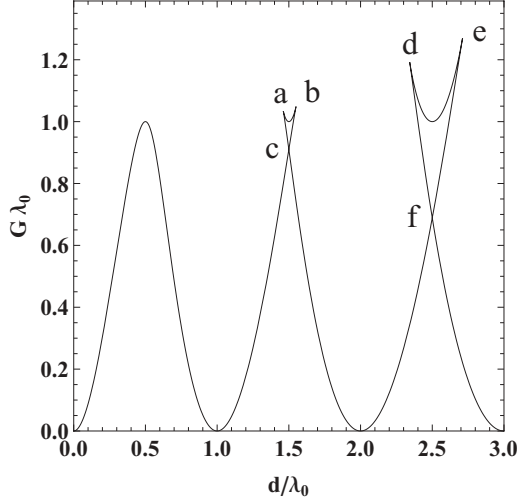


FIG. 7. CLC energy as a function of the cell thickness d/λ_0 for $L = \lambda_0$. When the thickness of the cell becomes larger than L multiple solutions appear and the pitch transitions become of first order. The branch between the cusp points a and b (d and e) represents unstable states.

Note that G'' is always positive for $L > d$; i.e., the surface twist angle ϕ_s varies continuously at the transition. In the case $L < d$, the system stability requires $L \geq -d \cos 2\phi_s$.

Figure 5 gives the spinodal lines (blue curves with a critical end point at $L = d$) for the case $L = \lambda_0$. The states inside the spinodal line are unstable and therefore the surface twist angle undergoes a discontinuity when the system crosses the spinodal. The ϕ_s jump is indicated by the dashed arrows in Fig. 5. The upward ($N \rightarrow N + 1$) and downward ($N + 1 \rightarrow N$) transitions occur at different values of the control parameter (d/λ_0) when $d > L$ as indicated by the position of the arrows in Fig. 5. Therefore, hysteresis loops are formed. The amplitude of the twist angle jump $\Delta\phi_s$ depends apparently on L and on d . In fact, a precise calculation shows that $\Delta\phi_s$ at the spinodal depends only on the L/d ratio and varies from 0, for $L \geq d$, up to $\pi/2$ for $L/d = 0$, i.e., for infinitely strong anchoring. For $L = 0$ the instability condition gives a jump of $\Delta\phi_s = \pi/2$ that happens at $\phi_s = N\pi \pm \pi/4$. Note that for a given CLC cell, if a jump of the surface twist angle is observed this should disappear when the thickness decreases (see Fig. 5).

Figure 7 shows the energy as a function of the reduced thickness d/λ_0 of the sample for $L = \lambda_0$. Changing the sample thickness, the stable states of the system for $d > L$ go through a crossing point. If the system evolves monotonically beyond the crossing point, it enters in a branch of metastable states that ends at a cusp point. On the upper curve between two cusp points the system becomes unstable (branches a and b). As is shown in Fig. 7, the critical thickness for $N \leftrightarrow N - 1$ pitch transition is $(N - 1/2)\lambda_0$. This result is obtained from the condition of equal energies in the two states at the transition, i.e.,

$$G_N = G_{N-1} \Rightarrow d_c^N / \lambda_0 = N - 1/2, \quad (20)$$

condition valid for all values of L and for each order $N = 1, 2, 3, \dots$ of the transition. Apparently, the critical thickness for the Ch-N transition is always $d_c = \lambda_0/2$ and independent

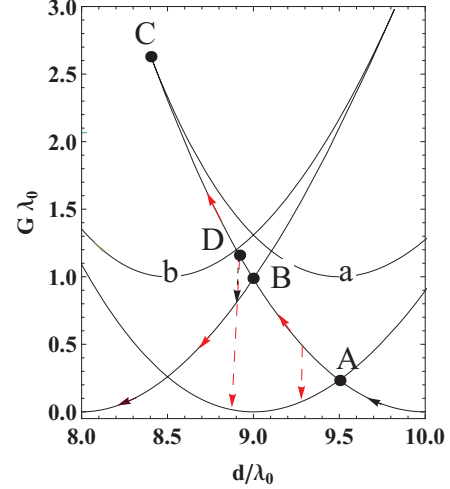


FIG. 8. (Color online) Energy vs d/λ_0 for $L/\lambda_0 = 1$. An unwinding transition with even multiplicity $m_p = 2$ between the states $N = 10$ and $N = 8$ is indicated by a red arrow at the point D. The branches a and b between successive cusp points represent unstable states.

on the form of the surface potential. This conclusion should originate from the topological nature of the transition. If transitions of higher multiplicity are of interest, one retrieves Eq. (12) for the critical thickness. For the RP potential, multiplicity and multistability are severely restricted from the condition given by Eq. (19). In the following we calculate the surface twist angle jump at the critical thickness, i.e., at the binodal for two limiting cases: $L = \infty$ and $L = 0$. In the limit $L \rightarrow \infty$, from Eq. (17) we get for the surface twist angle at d_c^N

$$\phi_s(d_c^N) = \frac{\pi}{\lambda_0} d_c^N = (2N - 1) \frac{\pi}{2}; \quad (21)$$

i.e., $\Delta\phi_s(d_c^N) = 0$ in the limit $L \rightarrow \infty$. In fact, $\Delta\phi_s(d_c^N) = 0$ for all $L \geq d$. The latter result is expected because the system has no instability when $L \geq d$. In the opposite case, when $L \rightarrow 0$, from Eq. (17), we get

$$\phi_s(d_c^N) = M\pi/2, \quad (22)$$

where M is an integer. For odd M , the obtained value corresponds to an unstable state. Therefore, $\phi_s(d_c^N) = N\pi$; i.e., $\Delta\phi_s(d_c^N) = \pi$ in the limit $L \rightarrow 0$.

Figure 8 shows the possibility of pitch transitions of higher multiplicity than one and of multistability. Suppose that initially the system is at the state with 10 half turns ($N = 10$). Under compression it could first transit to a state with $N = 9$ at a critical thickness $d_c^{10} = 9.5\lambda_0$, point A, but it can also enter in the metastable range ABC and transit directly to the state $N = 8$, either at the point B or at any point of the segment BC. Of course, the system can also have a transition towards the state with $N = 9$; i.e., in the segment BC the system exhibits bistability [10]. The latter case is illustrated at the point D where transitions to the states $N = 9$ and $N = 8$ are indicated by arrows. The cusp point C corresponds to the limit of metastability. In general, the multiplicity of the pitch transition increases with the order of the transition for fixed L and more generally with decreasing L/d . The

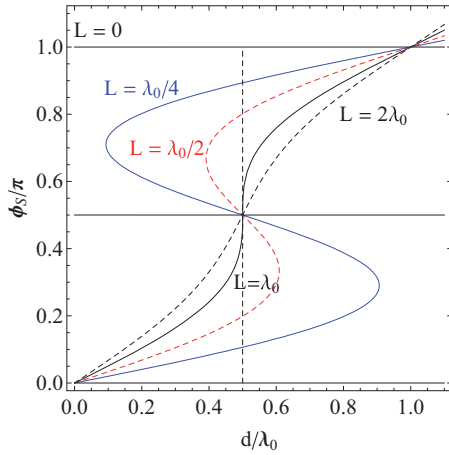


FIG. 9. (Color online) The surface twist angle ϕ_s , vs d/λ_0 for $L/\lambda_0 = 0, 0.25, 0.5, 1, 2$. The unwinding transition goes through a CP at $L/\lambda_0 = 1$. The middle part of each curve that has negative slope corresponds to unstable states. The vertical dashed line gives the transition points at the binodal. Once the transition has occurred the twist angle varies almost linearly with the thickness of the cell.

possibility to have transitions between states that differ by an even number of half turns (even multiplicity) has already been predicted [10] in both cases of a symmetric and an asymmetric cell and experimentally observed in [13]. Note that transitions with even multiplicity involve topologically equivalent configurations [10].

Finally, we investigate the Ch-N transition that takes place at $d_c^1 = \lambda_0/2$. Figure 9 shows ϕ_s as function of the reduced thickness d/λ_0 of the sample in the case $N = 1$, for $L/d = 0, 0.25, 0.5, 1, \text{ and } 2$. The surface twist angle ϕ_s glides continuously for $L \geq d$, as first predicted in [10] for the case of an asymmetric cell, and it presents an instability for $L < d$; i.e., there is a critical end point at $L = d$. The vertical dashed line indicates the position of the unwinding transitions towards the nematic phase, for $L < d$, defined from the equality of energy for both phases (Maxwell's rule). Note that for $L \neq 0$ the surface twist angle is different from zero even for very thin films for the $1 \rightarrow 0$ transition; i.e., it seems that the CLC phase persists ($\phi_s \propto d$).

V. DISCUSSION

Previous work on the strain induced pitch transitions in a CLC by Belyakov reposes on the assumption that the pitch transitions take place when $\phi_s = \pi/4$ for a RP potential [6,7]; i.e., the critical value of the surface twist angle is independent of the anchoring strength and it is constant. Therefore, the transition is always discontinuous. The critical thickness in [6,7] is calculated proportional to the surface extrapolation length $d_c = 2\pi L$, i.e., for an infinitely strong anchoring the cholesteric-nematic transition takes place for $d_c = 0$, while in the opposite limit $L \rightarrow \infty$, the critical thickness becomes infinite. These results are qualitatively and essentially different from our conclusions. In fact, the origin of the deviations between the two models is the

assumption of [6,7] that the condition for the transitions is imposed from the surface potential alone. In our approach the total energy of the system is minimized and the critical surface twist angle is found to vary with the reduced surface extrapolation length L/d , from $\phi_s = \pi/4$ for $L/d = 0$ to $\phi_s = \pi/2$ for $L/d = 1$ while there is no jump of ϕ_s for $L \geq d$. Therefore, the approach used in [6,7] should be valid in the limit where $L \rightarrow 0$. Nevertheless, even in this limit the critical thickness predicted by the two models is qualitatively different.

Let us now briefly investigate the role of the cell symmetry with respect to the interfaces. In the case of a symmetric cell where both interfaces are described by the RP potential and are both characterized by the same extrapolation length L the free energy simply takes the form

$$G = \left(\frac{2\phi_s}{d} - \frac{\pi}{\lambda_0} \right)^2 d + \frac{2}{L} \sin^2 \phi_s. \quad (23)$$

Then the spinodal is given by the equation $1 + \frac{d}{2L} \cos 2\phi_s = 0$, and the critical end point is localized at $d/L = 2$ or $L/d = 1$ with $L_c = L + L$. The critical thickness for the pitch transitions is always given by Eq. (20).

As shown above, the parabolic and the RP potential predict the same critical thickness for the Ch-N transition and in general for the pitch transitions. Nevertheless, the two models are not equivalent. In the parabolic model the pitch transition $\Delta\Phi/\pi = 1/(1 + L/d_c^N)$ is always of the first order but for $L = \infty$ where $\Delta\Phi = 0$. In general, the critical thickness does depend neither on the form of the surface potential nor from the symmetry of the two interfaces.

The position of the CP, that is at $L = d$ for the RP potential in the case of an asymmetric cell while at $L = d/2$ for the symmetric case and at $L = \infty$ for the parabolic potential, depends from the form of the potential itself and the symmetry of the cell. This means that one could choose experimentally the right potential by measuring L/d at the CP. Another method to determine the adequate surface potential is based on the calculation of the twist angle distribution in the cell [23]. A discussion on the instability mechanism of the pitch transition and the effect of fluctuations is reported in [9,10]. A transition between states that differ by an odd number of half-pitch ΔN requires the nucleation of defects and/or their propagation because the initial and final state are topologically incompatible. On the contrary, transitions between states with even ΔN do not require any defect. Therefore, transitions with $m_p = 1$ can be topologically blocked since the nucleation of a defect may require more energy than the energy gap for a transition with $m_p = 2$, for instance. In general, one expects that transitions with $m_p > 1$ are possible as far as the corresponding energy gap is smaller or of the same order of magnitude than the weaker anchoring energy that enters the problem. If anchoring is strong enough, then defect nucleation energy and/or defect propagation should give an upper limit for the pitch transition multiplicity and multistability.

VI. CONCLUSION

We have investigated the strain induced pitch transitions in a planar CLC cell with the helical axis perpendicular to the confinement plates. The easy axis on the plates are parallel, and out of plane director deviations are excluded. The critical thickness, where pitch transitions take place, does not depend

on the surface potential form and/or other material properties but the natural CLC pitch. The pitch transition is of topological nature with a critical end point. The position of the CP is model dependent via the ratio of the surface extrapolation length over the thickness of the cell, and it also depends on the symmetry of the cell with respect to the anchoring conditions.

-
- [1] P. G. de Gennes, *Solid State Commun.* **6**, 163 (1968).
 - [2] R. B. Meyer, *Appl. Phys. Lett.* **12**, 281 (1968).
 - [3] R. Dreher, *Solid State Commun.* **13**, 1571 (1973).
 - [4] P. J. Kedney and I. W. Stewart, *Lett. Math. Phys.* **31**, 261 (1994).
 - [5] P. J. Kedney and I. W. Stewart, *Continuum Mech. Thermodyn.* **6**, 141 (1994).
 - [6] V. A. Belyakov and E. I. Kats, *JETP* **91**, 488 (2000).
 - [7] V. A. Belyakov, *JETP Lett.* **76**, 88 (2002).
 - [8] V. A. Belyakov, I. W. Stewart, and M. A. Osipov, *Phys. Rev. E* **71**, 051708 (2005).
 - [9] S. P. Palto, *JETP* **94**, 260 (2002).
 - [10] A. D. Kiselev and T. J. Sluckin, *Phys. Rev. E* **71**, 031704 (2005).
 - [11] A. M. Scarfone, I. Lelidis, and G. Barbero, *Phys. Rev. E* **84**, 021708 (2011).
 - [12] I. Lelidis, G. Barbero, and A. M. Scarfone, *Cent. Eur. J. Phys.* **10**, 587 (2012).
 - [13] S. V. Belyaev and L. M. Blinov, *JETP Lett.* **30**, 99 (1979).
 - [14] P. Oswald, J. Baudry, and S. Pirkl, *Phy. Rep.* **337**, 67 (2000).
 - [15] L. J. M. Schlangen, A. Pashai, and H. J. Cornelissen, *J. Appl. Phys.* **87**, 3723 (2000).
 - [16] W. C. Yip and H. S. Kwok, *Appl. Phys. Lett.* **78**, 425 (2001).
 - [17] H. G. Yoon, N. W. Roberts, and H. F. Gleeson, *Liq. Cryst.* **33**, 503 (2006).
 - [18] I. I. Smalyukh, B. I. Senyuk, P. Palffy-Muhoray, O. D. Lavrentovich, H. Huang, E. C. Gartland, V. H. Bodnar, T. Kosa, and B. Taheri, *Phys. Rev. E* **72**, 061707 (2005).
 - [19] L. M. Blinov, *Structure and Properties of Liquid Crystals* (Springer, Berlin, 2001).
 - [20] M. Kleman and O. D. Lavrentovich, *Soft Matter Physics: An Introduction* (Springer, Berlin, 2002).
 - [21] A. Rapini and M. Papoular, *J. Phys. Colloques Paris* **30**, C4-54 (1969).
 - [22] P. G. de Gennes and J. Prost, *The Physics of Liquid Crystals* (Clarendon Press, Oxford, 1993).
 - [23] V. A. Belyakov, S. V. Semenov, and D. V. Shmeliova, *Mol. Cryst. Liq. Cryst.* **559**, 31 (2012).